

Liquid boron: X-ray measurements and *ab initio* molecular dynamics simulationsDavid L. Price,¹ Ahmet Alatas,² Louis Henet,¹ Noël Jakse,³ Shankar Krishnan,⁴ Alain Pasturel,³ Irina Pozdnyakova,¹ Marie-Louise Saboungi,⁵ Ayman Said,² Richard Scheunemann,⁶ Walter Schirmacher,⁷ and Harald Sinn^{2,8}¹*Centre de Recherche sur les Conditions Extrêmes et Matériaux: Haute Température et Irradiation, 45071 Orléans, France*²*Advanced Photon Source, Argonne National Laboratory, Argonne, Illinois 60439, USA*³*Laboratoire de Physique et Modélisation des Milieux Condensés, 38042 Grenoble, France*⁴*KLA-Tencor, San Jose, California 95134, USA*⁵*Centre de Recherche sur la Matière Divisée, 45071 Orléans, France*⁶*Containerless Research, Inc., Evanston, Illinois 60201, USA*⁷*Department für Physik, E13, Technische Universität München, 85747 Garching, Germany*⁸*DESY, Notkestrasse 85, 22607 Hamburg, Germany*

(Received 1 March 2009; published 1 April 2009)

We report results of a comprehensive study of liquid boron with x-ray measurements of the atomic structure and dynamics coupled with *ab initio* molecular dynamics simulations. There is no evidence of survival into the liquid of the icosahedral arrangements that characterize the crystal structures of boron but many atoms appear to adopt a geometry corresponding to the pentagonal pyramids of the crystalline phases. Despite similarities in the melting behavior of boron and silicon, there is little evidence of a significant structural shift with temperature that might suggest an eventual liquid-liquid phase transition. Relatively poor agreement with the observed damping of the sound excitations is obtained with the simple form of mode-coupling theory that has proved successful with other monatomic liquids, indicating that higher-order correlation functions arising from directional bonding and short-lived local structures are playing a crucial role. The large ratio of the high frequency to the isothermal sound velocity indicates a much stronger viscoelastic stiffening than in other monatomic liquids.

DOI: [10.1103/PhysRevB.79.134201](https://doi.org/10.1103/PhysRevB.79.134201)

PACS number(s): 61.25.Mv, 62.60.+v, 64.70.Ja, 61.05.cp

I. INTRODUCTION

Renewed interest in the structure and dynamics of classical liquids has been stimulated by two recent developments: the observation in both diffraction experiments¹ and numerical simulations²⁻⁴ of first-order liquid-liquid phase transitions (LLPT) between a high-density and low-density phase, and the success of a relatively simple version of mode-coupling theory (MCT) in explaining the dynamics of simple liquids.^{5,6} In both cases the details of the interatomic potential are important: the occurrence of a liquid-liquid transition appears to require a potential with either two distinct short-range repulsive distances⁷ or a repulsive soft core⁸ while the MCT seems to work best if the potential can be approximated by a smoothed hard-sphere interaction.⁶

Relatively little is known about liquid boron due in part to its high melting point. The existence in the solid of α -rhombohedral and β -rhombohedral crystal structures, which can be regarded as high-density and low-density phases,^{9,10} suggests the possibility of high-density and low-density phases in the liquid. Furthermore, the presence of icosahedra and pentagonal pyramids in both solid phases implies that two length scales are involved. The possibility of their survival on melting—as has been found for complex structural units in other semiconducting systems, for example, NaSn (Ref. 11) and CsPb (Ref. 12)—might be invoked to explain the unusual properties of the liquid. Boron contracts on melting,¹³ exhibits an increase—albeit small—in the electrical conductivity,¹⁴ and—as we shall show—shows a considerable decrease in the longitudinal sound velocity, properties similar to silicon and germanium

in which substantial evidence exists for an LLPT on extreme supercooling.^{2,15,16} Like Si and Ge, B is a semiconductor under ambient conditions but transforms to a superconducting metal under pressure¹⁷ and a recently discovered ionic form at even higher pressure.¹⁸ While the potential in the solid is clearly far from a hard-sphere interaction, it is likely to be more isotropic in the liquid, and the applicability of the simple MCT approach cannot be ruled out *a priori*. In order to address these questions we have made a comprehensive study of liquid boron with x-ray measurements of the atomic structure and dynamics coupled with *ab initio* molecular dynamics (AIMD) simulations, and relate these to the physical and electrical properties of the liquid in cases where these are known.

II. EXPERIMENTAL DETAILS

Crystalline boron exhibits a remarkable variety of structures, composed of icosahedra and pentagonal pyramids, and characterized by large unit cells. The stable form at low temperature is either the α -rhombohedral⁹ or a symmetry-broken β -rhombohedral¹⁹ structure, and at high temperature the β rhombohedral. It melts into a stable liquid at 2360 ± 10 K, a temperature that is readily accessible with present-day levitation techniques.²⁰ We measured its structure using a combination of conical nozzle levitation, laser heating, and x-ray diffraction (XRD) at the 12-ID-B beam line at the Advanced Photon Source (APS) with an incident energy of 21 keV. The experimental methods and data analysis procedures were those used previously for liquid Al_2O_3 ,²¹ Si,²² and SiGe.²³ The present measurements were made on samples of 2.5 mm

diameter prepared from 99.9995% pure boron; the O₂ and N₂ content of the Ar levitation gas was estimated to be <0.01 ppm. Temperatures were controlled to within 10 K and measured with two pyrometers directed at the location on the sample where the x-ray beam was incident, with an estimated uncertainty of 15 K. The diffracted intensity was determined over a 2θ angular range of 2° – 110° , giving a scattering vector Q range of 0.7 – 17 \AA^{-1} with a resolution of 0.02 \AA^{-1} . The Q range, statistics, and systematic accuracy were considerably enhanced over an earlier measurement.²⁴ The structure factor was derived from the relation $S(Q) = I_{\text{coh}}(Q)/f^2(Q)$, where $I_{\text{coh}}(Q)$ is the normalized coherent scattering intensity and $f(Q)$ the scattering amplitude. The pair-correlation function $g(r)$ was obtained from $S(Q)$ by the usual Fourier transform, with a Lorch modification function to reduce the effect of the truncation at 17 \AA^{-1} . Number densities at each temperature were derived from the recent measurements of Paradis *et al.*¹³

AIMD simulations were carried out with the augmented-wave projector²⁵ and the Perdew-Wang generalized gradient approximation²⁶ as implemented in the VASP code.^{27,28} The $2s$ and $2p$ orbitals of boron were treated as valence orbitals with a plane-wave cutoff of 300 eV. The simulations were carried out in the NVT ensemble with a Nosé thermostat, and the Verlet algorithm was used with a time step of 3 fs and a cubic cell of 256 atoms subject to standard periodic boundary conditions. Only Γ -point sampling was considered. In this formulation, the only experimental input is the density, again taken from Ref. 13. Starting at from a well-equilibrated state 2600 K, the system was quenched instantaneously at 2400 K at constant volume and after 2 ps was compressed to the experimental density. After an equilibration period of 2 ps, configurations were extracted at each temperature to produce averaged quantities, with a typical run duration of 30 ps. These large simulation cells and duration are needed to calculate accurately the static and dynamic structure factors down to $Q=0.5 \text{ \AA}^{-1}$, and represent a substantial improvement over the previous AIMD of Vast *et al.*²⁹

The dynamics were measured by inelastic x-ray scattering (IXS) at the 3-ID-C beam line³⁰ at the APS with an x-ray energy of 21.6 keV and full width at half maximum energy resolution of 1.9 meV. The experimental methods and analysis procedures were those used previously for liquid Al₂O₃,³¹ Si,³² and Ti,⁵ and the samples and environmental conditions were similar to those of the XRD measurements. The liquid temperature was maintained at 2340 K, and measurements were also made in the β -crystalline phase at 2220 K. IXS spectra were collected over an energy-transfer ($E=\hbar\omega$) range of -10 – $+80$ meV for Q 's between 0.1 and 0.6 \AA^{-1} , and over a smaller range of -15 to $+15$ meV for Q 's up to 2.8 \AA^{-1} . The background was determined from the measurement with the hot solid. The scattering function $S(Q, \omega)$ and the current correlation function $C(Q, \omega) = \omega^2 S(Q, \omega) / Q^2$ were derived from the measured intensity $I(Q, \omega)$ through the relation

$$I(Q, \omega) = I_0 \int \frac{k_B T}{\exp[\hbar(\omega - \omega')/k_B T]} S(Q, \omega - \omega') R(\omega') d\omega', \quad (1)$$

where the normalizing factor I_0 was determined from the second-moment relation.

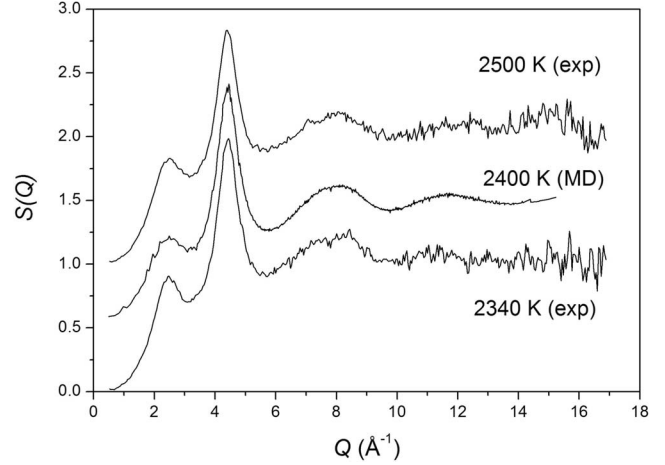


FIG. 1. Structure factor for liquid boron measured by XRD at 2500 and 2340 K, together with the AIMD result for 2400 K. The experimental result at 2500 K is displaced upward by 1.0 for clarity.

III. RESULTS

Figure 1 shows the XRD results for $S(Q)$ in the normal and slightly undercooled liquids, together with the AIMD result obtained from a direct formulation in Q space. All $S(Q)$'s show well-defined peaks at $Q=2.5$ and 4.4 \AA^{-1} , and weaker ones at 8 and 11.8 \AA^{-1} . Scaling with the nearest-neighbor distance $r_1=1.77 \text{ \AA}$, the first two peaks have Qr_1 values of 4.5 and 7.9, respectively: the first is typical of the first peak position in elemental semiconducting glasses and liquids while the second is a typical value for packing of hard spheres.³³ Figure 2 shows the corresponding $g(r)$'s. The experimental $g(r)$ is fitted well by Gaussian peaks centered at 1.77, 3.13, 4.58, 6.08, and 7.56 \AA , and the same peaks can be distinguished in the AIMD. The AIMD and XRD results are in excellent agreement in both Q and r spaces. The inset

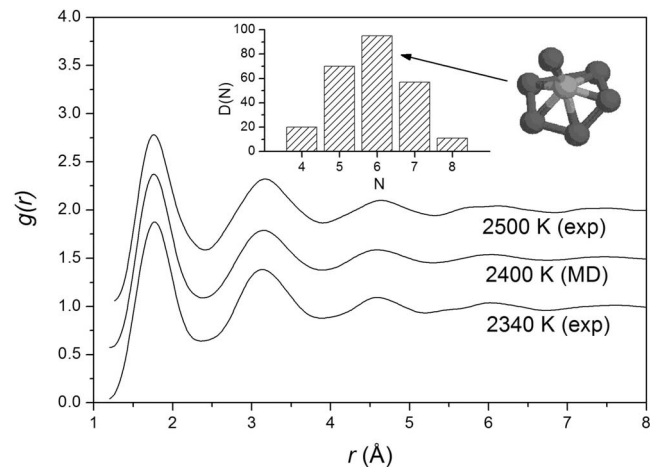


FIG. 2. Pair correlation function measured by XRD at 2500 and 2340 K, compared with the AIMD result for 2400 K, broadened by the Fourier transform of the Lorch modification function. Successive curves are displaced upward by 0.75 for clarity. Inset: distribution of coordination numbers (defined within a radius of 2.37 \AA) from the AIMD at 2400 K, and a typical sixfold-coordinated atom showing a pentagonal pyramid configuration.

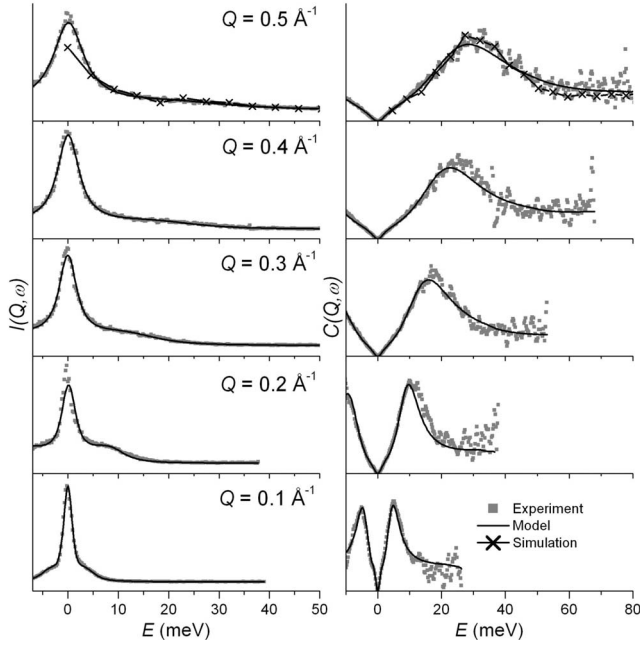


FIG. 3. IXS spectra $I(Q, \omega)$ (left) and current correlation function $C(Q, \omega) = \omega^2 I(Q, \omega) / Q^2$ (right) at 2370 K. The solid lines represent a fit with the two-relaxation-time model described in the text. The crosses show the AIMD result at 0.5 \AA^{-1} , the lowest Q value studied in the simulation.

of Fig. 2 shows a typical distribution of nearest-neighbor coordination numbers obtained from the AIMD, in which sixfold-coordinated atoms are the most numerous. The average coordination number calculated from the area of the first peak in both the XRD and the AIMD $g(r)$'s is 6.0, compared with 6.5 and 6.4 in the α -rhombohedral and β -rhombohedral crystals, respectively. The peaks in the AIMD $S(Q)$ and $g(r)$ sharpen up on cooling down to and below the equilibrium melting point but there are no systematic temperature shifts in their positions or coordination numbers.

The results for $I(Q, \omega)$ and $C(Q, \omega) = \omega^2 I(Q, \omega) / Q^2$ at the five lowest Q values are shown in Fig. 3. The solid lines represent the phenomenological model discussed below. The AIMD and IXS Q ranges overlap only at 0.5 \AA^{-1} where the AIMD result is seen to be in reasonable agreement with the experimental data.

The nanometer distance scale presents a challenge for the dynamical theory of liquids, being intermediate between the regions where hydrodynamics and kinetic theory may be expected to be valid.^{34,35} As a first approach, we made model calculations in the framework of generalized hydrodynamics, in which the scattering function is written as

$$S(Q, \omega) = \frac{S(Q)}{\pi} \text{Re} \left[i\omega + \frac{\omega_0^2}{i\omega + M(Q, \omega)} \right]^{-1}, \quad (2)$$

where $\omega_0^2 = k_B T Q^2 / m S(Q)$ is the second frequency moment of $S(Q, \omega) / S(Q)$, and m being the atomic mass. The low- Q data were fitted with the phenomenological memory function³⁵

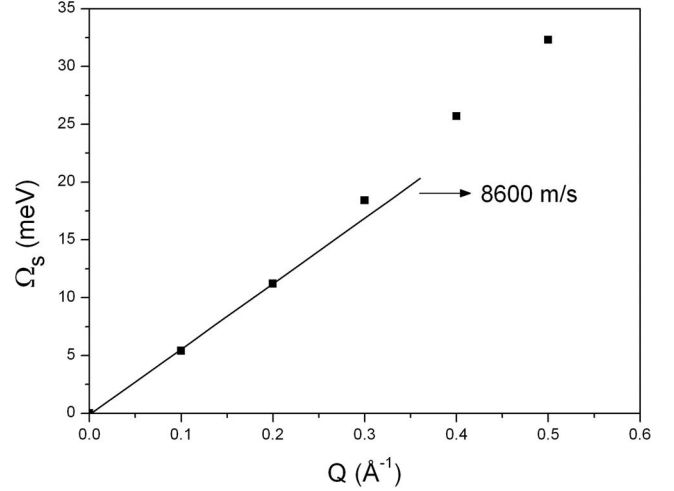


FIG. 4. Dispersion of the sound excitations. The frequencies $\Omega_s(Q)$ are obtained from the maxima in $C(Q, \omega)$ as a function of ω .

$$M(Q, t) = \Delta_1^2 e^{-t/\tau_1} + \Delta_2^2 e^{-t/\tau_2}, \quad (3)$$

where the relaxation times τ_1 and τ_2 , and relaxation strengths Δ_1 and Δ_2 are treated along with ω_0^2 as fit parameters. The low- Q spectra could be fitted with very similar relaxation times: $\tau_1 = 0.3 \pm 0.1$ and $\tau_2 = 0.025 \pm 0.02$ ps, and a ratio $\Delta_1 / \Delta_2 = 0.35 \pm 0.05$. The fit gives a value for $S(Q)$ of 0.068 ± 0.01 for all Q 's in the range of 0.2 – 0.5 \AA^{-1} , consistent with the low- Q limit of the AIMD. The corresponding value for the isothermal sound velocity $v_i = \omega_0 / Q$ is 5300 ± 200 m/s. The dispersion of the sound excitations, shown in Fig. 4, was derived by plotting the maxima $\Omega_s(Q)$ in $C(Q, \omega)$ against Q , giving a high-frequency sound velocity $v_s = \omega_s(Q) / Q$ of 8600 ± 300 m/s. The corresponding value obtained for the hot solid at 2170 K was $14\,000 \pm 300$ m/s, consistent with the reported value of $14\,300$ m/s at room temperature.³⁶ The large ratio (1.6 ± 0.1) of the high frequency to the isothermal sound velocity in the liquid, compared with the values of 1.1–1.2 found in other monatomic liquids,³⁵ indicates an unusually strong viscoelastic stiffening. The upturn of the dispersion around 0.25 \AA^{-1} is due to the fast viscoelastic relaxation process described by τ_2 .

IV. DISCUSSION

The issues stated in Sec. I raise the question of the survival into the liquid of the icosahedron and pentagonal pyramidal structural units of the crystalline phases. Icosahedra would produce a first sharp diffraction peak³³ around 0.8 \AA^{-1} , and indeed such a peak was observed in diffraction measurements on solid amorphous boron.³⁷ There is no evidence of such a peak in either the XRD or AIMD results, and no complete icosahedral arrangements are found in the simulation. On the other hand, many atoms adopt with their first neighbors a geometry corresponding to the pentagonal pyramids of the crystalline phases, shown in the inset of Fig. 2.

The generalized longitudinal viscosity can be related through the Green-Kubo relations to the density correlations. It was extracted from the IXS data in the low Q region by the relation³⁸

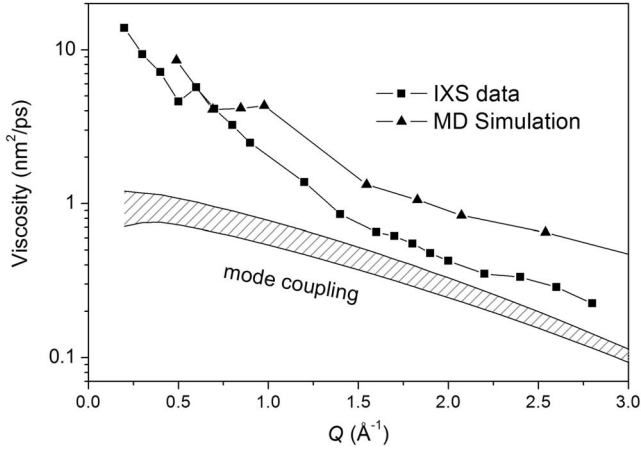


FIG. 5. Experimental values of generalized longitudinal kinematic viscosity η_l/ρ obtained from the IXS measurements (solid circles) and AIMD simulations (solid triangles). The continuous lines bounding the hatched area represent the results of a mode-coupling theory calculation with two different ways of treating the high- Q data.

$$\eta_l(Q) = \frac{\pi\rho v_0^2 S(Q, \omega=0)}{S(Q)^2} = \frac{\rho(\Delta_1^2 \tau_1 + \Delta_2^2 \tau_2)}{Q^2}, \quad (4)$$

where ρ is the mass density and $v_0^2 = k_B T/m$, using values obtained from fit of Eq. (3). The right-hand side of Eq. (4) applies to the viscoelastic model introduced in Eqs. (2) and (3). For the higher Q values—0.6–2.8 \AA^{-1} —where the central peak dominates, a single Lorentzian function was fitted to the data and $S(Q,0)/S(Q)$ was determined from its width. The result is plotted as η_l/ρ in Fig. 5, together with the values obtained from the AIMD results for $S(Q,0)/S(Q)$. The agreement is good at low Q but, at Q 's around the peak of $S(Q)$, the AIMD predicts a higher value, indicating a narrower shape to $S(Q, \omega)$. The value extrapolated to low Q , $\eta_l = 15$ mPa s, is appreciably higher than in alkali metals but only slightly higher than other group-13 metals, Al and Ga.³⁵

We now address the applicability of the density-fluctuation version of MCT, previously employed successfully to describe the glass transition in liquids^{39,40} and more recently to the dynamics of liquids in equilibrium,^{5,6} to liquid boron. The generalized longitudinal viscosity obtained from the application of the MCT to the memory function in Eq. (3) is shown by the hatched area in Fig. 5, where the two lines bounding the hatched area represent two different ways of treating the high- Q data, which also affect the result at low Q . It can be seen that the calculation is in reasonable agreement at higher Q but fails by an order of magnitude at low Q . This comparison contrasts with the excellent agreement over an extended Q range, 0.8–3.0 \AA^{-1} , obtained with a similar calculation for liquid Ti.⁵ The poor agreement obtained here for boron indicates that higher-order correlation functions arising from the directional bonding and short-lived local structures observed in the AIMD simulations are playing a crucial role in the damping of the sound excitations.

Finally, we return to the question of an LLPT in boron. As discussed earlier, it is tempting to raise the comparison with silicon since boron shows a contraction on melting [3% compared with 11% in Si (Refs. 41–44)], accompanied by a considerable decrease in longitudinal sound velocity [45%, compared with 42% in Si (Ref. 32)]. On the other hand the entropy increase on melting is only 9.6 J mol⁻¹ K⁻¹, a typical value for most elements, while it is three times larger for Si and Ge.⁴⁵ As we have seen, the change in structure (decrease in $\sim 8\%$ in coordination number compared with increase in $\sim 50\%$ in Si) is relatively modest, as is that in the conductivity (increase¹⁴ of 510 $\Omega^{-1} \text{cm}^{-1}$ compared with $\sim 10^4$ $\Omega^{-1} \text{cm}^{-1}$ in Si). Furthermore, there is little evidence of a significant structural shift with temperature as found in our previous studies of silicon²² that might suggest an eventual phase transition.² This suggests that melting in boron is more similar to the transition between solid and supercooled tetrahedral liquid Si predicted by the computer simulations,² and that any LLPT must take place, if at all, at appreciably higher temperature.

V. CONCLUSIONS

While liquid boron is characterized by a short-range order that resembles that of the stable crystal phases, neither the XRD measurements nor the AIMD simulations find evidence of survival into the liquid of the icosahedral arrangements that characterize the crystal structures. The simulations do, however, reveal a significant number of atoms that adopt with their first neighbors a geometry corresponding to the pentagonal pyramids of the crystalline phases. Furthermore, there is little evidence of a significant structural shift with temperature that might suggest an eventual liquid-liquid phase transition at high supercooling.

The liquid dynamics in the nanometer wavelength scale probed in the IXS measurements can be satisfactorily fit with a phenomenological model incorporating two-relaxation times that has been previously used for other monatomic liquids. The large ratio of the high frequency to the isothermal sound velocity, however, indicates an unusually strong viscoelastic stiffening. Poor agreement with the observed damping of the sound excitations is obtained with the simple form of mode-coupling theory that has proven successful with other monatomic liquids, indicating that higher-order correlation functions arising from directional bonding and short-lived local structures are playing a crucial role.

ACKNOWLEDGMENTS

We thank M. A. Beno and J. Linton of the APS for their help with the XRD experiments, J. Rix for assistance with the experimental hardware, and C. A. Angell, C. Chatillon, and F. Millot for useful discussions. The work was supported in part by a grant from the NASA Microgravity Sciences and Applications Division, Grant No. NAS8-00122. Work at the APS is supported by the U.S. Department of Energy, Office of Science, Office of Basic Energy Sciences, under Contract No. DE-AC02-06CH11357.

- ¹Y. Katayama, Y. Inamura, T. Mizutani, M. Yamakata, W. Utsumi, and O. Shimomura, *Science* **306**, 848 (2004).
- ²C. A. Angell and S. S. Borick, *J. Phys.: Condens. Matter* **11**, 8163 (1999).
- ³S. Sastry and C. A. Angell, *Nature Mater.* **2**, 739 (2003).
- ⁴N. Jakse and A. Pasturel, *Phys. Rev. Lett.* **99**, 205702 (2007).
- ⁵A. H. Said, H. Sinn, A. Alatas, C. A. Burns, D. L. Price, M. L. Saboungi, and W. Schirmacher, *Phys. Rev. B* **74**, 172202 (2006).
- ⁶W. Schirmacher and H. Sinn, *Condens. Matter Phys.* **11**, 127 (2008).
- ⁷G. Franzese, G. Malescio, A. Skibinsky, S. V. Buldyrev, and H. E. Stanley, *Nature (London)* **409**, 692 (2001).
- ⁸A. Skibinsky, S. V. Buldyrev, G. Franzese, G. Malescio, and H. E. Stanley, *Phys. Rev. E* **69**, 061206 (2004).
- ⁹A. Masago, K. Shirai, and H. Katayama-Yoshida, *Phys. Rev. B* **73**, 104102 (2006).
- ¹⁰M. J. van Setten, M. A. Uijttewaal, G. A. de Wijs, and R. A. de Groot, *J. Am. Chem. Soc.* **129**, 2458 (2007).
- ¹¹M.-L. Saboungi, J. Fortner, W. S. Howells, and D. L. Price, *Nature (London)* **365**, 237 (1993).
- ¹²D. L. Price, M.-L. Saboungi, R. Reijers, G. Kearley, and R. White, *Phys. Rev. Lett.* **66**, 1894 (1991).
- ¹³P.-F. Paradis, T. Ishikawa, and S. Yoda, *Appl. Phys. Lett.* **86**, 151901 (2005).
- ¹⁴B. Glorieux, M.-L. Saboungi, and J. E. Enderby, *Europhys. Lett.* **56**, 81 (2001).
- ¹⁵G. Kresse and J. Hafner, *Phys. Rev. B* **49**, 14251 (1994).
- ¹⁶A. Filipponi and A. Di Cicco, *Phys. Rev. B* **51**, 12322 (1995).
- ¹⁷M. I. Eremets, V. V. Struzhkin, H.-K. Mao, and R. J. Hemley, *Science* **293**, 272 (2001).
- ¹⁸A. R. Oganov, J. Chen, C. Gatti, Y. Ma, Y. Ma, C. W. Glass, Z. Liu, T. Yu, O. O. Kurakevych, and V. L. Solozhenko, *Nature (London)* **457**, 863 (2009).
- ¹⁹M. Widom and M. Mihalkovic, *Phys. Rev. B* **77**, 064113 (2008).
- ²⁰S. Krishnan and D. L. Price, *J. Phys.: Condens. Matter* **12**, R145 (2000).
- ²¹S. Krishnan, L. Hennem, S. Jahn, T. A. Key, P. A. Madden, M.-L. Saboungi, and D. L. Price, *Chem. Mater.* **17**, 2662 (2005).
- ²²N. Jakse, S. Krishnan, E. Artacho, T. Key, L. Hennem, B. Glorieux, A. Pasturel, D. L. Price, and M.-L. Saboungi, *Appl. Phys. Lett.* **83**, 4734 (2003).
- ²³S. Krishnan, L. Hennem, T. Key, B. Glorieux, M.-L. Saboungi, and D. L. Price, *J. Non-Cryst. Solids* **353**, 2975 (2007).
- ²⁴S. Krishnan, S. Ansell, J. Felten, K. J. Volin, and D. L. Price, *Phys. Rev. Lett.* **81**, 586 (1998).
- ²⁵G. Kresse and D. Joubert, *Phys. Rev. B* **59**, 1758 (1999).
- ²⁶Y. Wang and J. P. Perdew, *Phys. Rev. B* **44**, 13298 (1991).
- ²⁷G. Kresse and J. Furthmüller, *Comput. Mater. Sci.* **6**, 15 (1996).
- ²⁸G. Kresse and J. Furthmüller, *Phys. Rev. B* **54**, 11169 (1996).
- ²⁹N. Vast, S. Bernard, and G. Zerah, *Phys. Rev. B* **52**, 4123 (1995).
- ³⁰H. Sinn, *J. Phys.: Condens. Matter* **13**, 7525 (2001).
- ³¹H. Sinn, B. Glorieux, L. Hennem, A. Alatas, M. Hu, E. E. Alp, F. J. Bermejo, D. L. Price, and M.-L. Saboungi, *Science* **299**, 2047 (2003).
- ³²A. Alatas, A. H. Said, H. Sinn, E. E. Alp, C. N. Koditwakku, B. Reinhart, M.-L. Saboungi, and D. L. Price, *J. Phys. Chem. Solids* **66**, 2230 (2005).
- ³³D. L. Price, S. C. Moss, R. Reijers, M.-L. Saboungi, and S. Susman, *J. Phys.: Condens. Matter* **1**, 1005 (1989).
- ³⁴D. L. Price, M.-L. Saboungi, and F. J. Bermejo, *Rep. Prog. Phys.* **66**, 407 (2003).
- ³⁵T. Scopigno, G. Ruocco, and F. Sette, *Rev. Mod. Phys.* **77**, 881 (2005).
- ³⁶D. Gerlich and G. A. Slack, *J. Mater. Sci. Lett.* **4**, 639 (1985).
- ³⁷R. G. Delaplane, T. Lundstrom, U. Dahlborg, and W. S. Howells, in *Boron-Rich Solids*, AIP Conference Proceeding No. 231, edited by D. Emin, T. L. Aselage, A. C. Switendick, B. Morosin, and C. L. Beckel (AIP, New York, 1991), p. 241.
- ³⁸A. A. Kugler, *J. Stat. Phys.* **8**, 107 (1973).
- ³⁹U. Bengtzelius, W. Götze, and A. Sjölander, *J. Phys. C* **17**, 5915 (1984).
- ⁴⁰W. Götze, in *Liquids, Freezing and the Glass Transition*, edited by J.-P. Hansen, D. Levesque, and J. Zinn-Justin (North-Holland, Amsterdam, 1991).
- ⁴¹K. Ohsaka, S. K. Chung, W. K. Rhim, and J. C. Holzer, *Appl. Phys. Lett.* **70**, 423 (1997).
- ⁴²S. Kimura and K. Terashima, *J. Cryst. Growth* **180**, 323 (1997).
- ⁴³M. Langen, T. Hibiya, M. Eguchi, and I. Egry, *J. Cryst. Growth* **186**, 550 (1998).
- ⁴⁴H. Sasaki, E. Tokizaki, K. Terashima, and S. Kimura, *Jpn. J. Appl. Phys., Part 1* **33**, 3803 (1994).
- ⁴⁵*Smithells Metals Reference Book*, edited by E. A. Brandes (Butterworth, London, 1983), p. 8-2.